

JACtree: An Orthotropical-Radial approach to Brain Structural Connectivity

Marino Davolos Julián*, Arias Haro Cruz and Jefferies Elizabeth

Department of Psychology and York Neuroimaging Centre, University of York, YO10 5DD York, UK

Introduction

The orthotropic-radial approach

JACtree performs an exhaustive analysis of the radial microstructure of white matter tracts (WMTs). Considering the topology of the canonical WMTs, it is also appropriate to describe it as transversal (instead of radial). However, the radial concept is preserved because the topology of biological material, such as WMTs, is orthotropic, not uniaxial. In this way, each canonical WMT can be considered a deformed configuration of a tubular structure. A canonical WMT is a bundle of compact, axonal fibers, recognizable by their shape, included in WMT atlases classification. Canonical WMTs have a recognizable nomenclature, and regardless of differences between researchers, there were ten canonical WMTs described in Catani & Thiebaut de Schotten [1,2] listed seven canonical WMTs but they applied a restricted criterion regarding the canonical WMTs, opening the gate of subdivisions. With the development of new atlases, the number of WMTs increased to fifteen [3,4], and still spherical deconvolutions allow to include U-shaped fibers, exponentially increasing their number to over a hundred. However, previous atlases assume different technology and hence different criteria: the new releases include short fibers, raise to develop gray matter tractography, sheetography [5], accompanied by increasing magnetic resonance (MR) capacity as well as novel mathematical models for MR reading out process. Currently, canonical WMTs are easily differentiated from U-shaped fibers, that are 20-30 times inferior in volume [6], the traditional DTI models growth in impossibility to detect the spectrum of WMTs proposals [7]. The classic canonical WMTs are anatomically labeled, recognizable by perception (commonly cited as 'hook form', 'diagonal strip form'), while subdivisions are the main root of differences; this is a taxonomical organization fact [8].

JACtree represents an orthotropical-radial approach to brain structural connectivity based on findings of radial heterogeneity and regularities in that phenomena in the main WMTs. Also, results applying JACtree were satisfactory enough to encourage the development of a toolset to explore with solid mathematical and physics fundaments this approach. After performing seventeen pilot studies using different databases from countries and varied age [9-11] we found a pattern of eccentricity of internal WMTs. Hence, segmentation with longitudinal and radial criteria allow to replicate experiments previously analyzed without the radial dimension into account. Correlations were higher in significance, locations acquired precision, mean diffusion (MD) and fractional anisotropy (FA) coefficients reached a theoretical coherent relation. It was clear in longitudinal databases [12,13], where firstly a cognitive process has significant correlations with MD, anticipating stronger cognitive-process to FA correlations. In this work we found

a correlation between the inferior longitudinal fasciculus (ILF) and phonological awareness with twice the strength of that reported from the original authors [$r=0,512$, $p<0,0001$] [13] at the same time the longitudinal data allows to follow that correlations migrate from ILF-occipital to ILF-middle temporal segments, specifically to medial rings (JACtree Contractio tool cluster the radial ILF in three rings).

Meanwhile the aforementioned development of gray matter and U-shaped short fibers tractography are in progress, this new radial-orthotropic approach allows to explore also short fibers. For the moment it is only necessary to point out that the organization of both forms of white matter presentation are distant in topology enough to consider CSD-sheetography techniques (especially the last) as a different class of brain connectivity analysis. However, results to date are tentative, serving as an orientation or horizon for the establishment of a technique. Conceptually it is still a set of conjectures that do not reach the level of hypothesis.

Objectives

a. The objective presented in Part A is to set the basics of JACtree. The relevant antecedents supporting this approach demanded a collection of different disciplines that suggest the radial heterogeneity of WMTs coming from such far applications. Balo's multiple sclerosis is a dominant white matter disease in China [14,15]. They directly establish the concept of orthotropical-radial organization of WMTs. This disease is characterized because it follows the inverse phenomenology of "Western" multiple sclerosis: the myelin shield is intact, but an implosion in the WMTs trigger the symptoms. They considered there are different pressures of FA|MD into the WMTs, hypothesizing what we did: a radial heterogeneity with regularities that form part of the WMT organization development. In single nerve experiments coherent radial ATP signals were never found after data analysis using Fourier transformation [16]. In other experiment, using MR elastography, Romano, *et al.* [17] formulated the 'flexible-forced by orthogonal vectors' concept to describe WMTs material. They detected that curvature of WMTs increase the entropy of brain structural communication, specially related with aging.

b. The objective presented in Part B is to show a set of experiments linked to uncinate fasciculus (UF), to compare results applying JACtree versus uniaxial *motus non cooperante* (mnc) (non-radial approach)

*Correspondence to: Marino Davolos Julián, Department of Psychology and York Neuroimaging Centre, University of York, YO10 5DD York, UK, E-mail: juliancarlosmarino.davolos@york.ac.uk

Received: March 29, 2021; Accepted: April 15, 2021; Published: April 19, 2021

to the same databases. This WMT was chosen to center the different pipeline JACtree consequences to only one canonical WMT. The radial divisions and longitudinal segmentations would be extra-limited if more than one WMT would be in the spot.

Part A

Materials and methods

Magnetic Resonance Diffusion data pipeline

Diffusion Data (DD)-MR acquisitions are the raw material of this application. Tractography based on data coming from the MR readout stored in voxels is the manufacture. The extraction of WMTs based on streamlines determined by the use of Boolean operators is the technology of JACtree. The information coding computer platform requires the processing of linear algebra of matrices. JACtree works in dialogue with ExploreDTI. The rationale for this decision can be found in the work of Bach, *et al.* [18], also developments of Colby, *et al.* [19] in along tract analysis, the specifications stated by Lebel, *et al.* [20] about Atlas Based Tract Segmentation. All of these works used ExploreDTI rationale, which can be summarized in a high-developed control of physics artifacts conjoint to work over the brain native space, excluding skeletonizations and the rest of shortcuts, which consume less time but ExploreDTI privileges that the computational representation is adjusted to the native brain reference space, even if the time is longer [21].

Rationale to determine radial organization of White Matter Tracts

JACtree Contractio tool computes WMTs FA|MD radial microstructure. In brief, significant FA heterogeneity is the alternative hypothesis, whereas FA homogeneity is the null hypothesis. The JACtree tool calculates the microstructure (FA|MD) encompassing a possible orthotopical eccentricity, which include a) radial significant concentricity b) radial significant ax-centricity c) homogeneity- uniaxial (*mnc*). The steps were programmed in matrix informatic language, at following the main concepts will be described in a global to local order:

JACtree is based on streamlines tractography post- processing [22,23]. (Figure 1) shows a whole brain streamline based tractography.

JACtree Contractio tool divide dissected WMTs (UF in this case) in N_x (nine by default) similar longitude segmented rings. To understand this process is necessary to clear sub-steps, proper of streamline based tractography [24]. The whole brain tractography is an Euclidean Space disposed to be fulfilled by minimal information points (Figure 2). The quantity of information points depends on resolution quality, the voxel size in MR. Once the WMT was extracted, it is saved as a matrix. As (Figure 3) shows, the UF is into an Euclidean space also. The information of connectivity depends on the readout of MR-DD that stored the information in minimum acquisition units (voxels) on a Field of View (FOV).

The key concept here is to assign a scalar to each voxel, important is that JACtree needs to assign a number, not a coordinate combination of three numbers [X,Y,Z] to each information point in the FOV. Then, is necessary to understand what means the FOV, because JACtree operate with a particular algorithm system to assign the scalars to what is a FOV coordinate. That is the cornerstone to calculate Euclidean distances applied to the points of information, allowing to determine radial distances inside the WMT. In the acquisition process the brain native space (also called participant) is positioned in a comfortable stretcher. From the central computers locators brain native spaces are

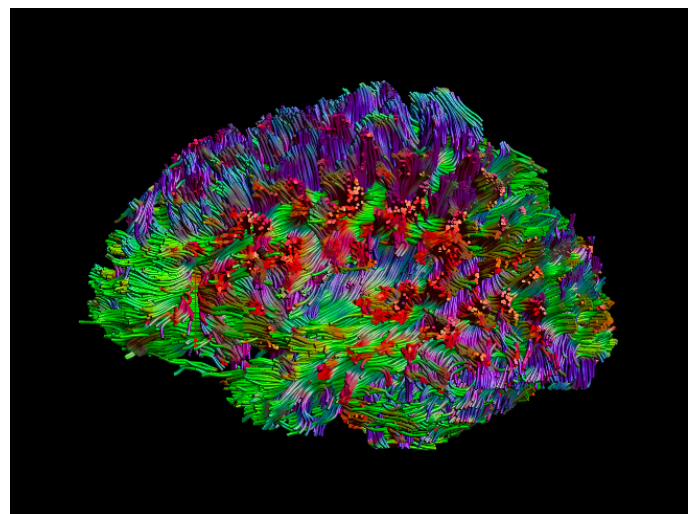


Figure 1. Whole brain streamline based tractography. Colors correspond to international Fiber Encoding of Fractional Anisotropy (FEFA). To extract a WMT (UF in this example) Boolean operators AND, NOT, OR are applied, as shown in Figure 2

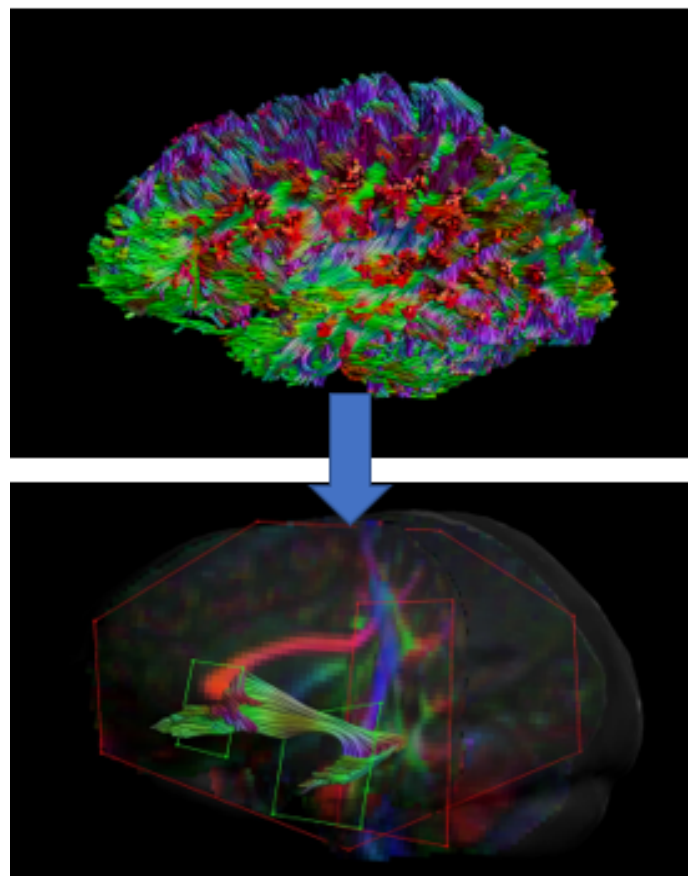


Figure 2. The whole brain tractography (upper) contains all minimal microstructure informative points. The image below exhibits Boolean operators to extract Uncinate Fasciculus.

placed that center target in a Euclidean Space-cube. FOV includes the brain parenchyma and cerebellum, that three-dimensional box has empty space [Not a Number] (NaN). In MR-DD process the structural connectivity values enter within the FOV space in the reading out meeting between a) main magnetic field of MR, b) the head coil, c) the channels inside the head coil and d) the electromagnetic spins of the

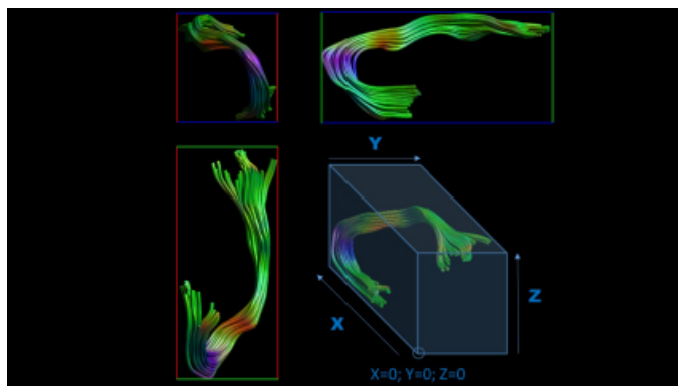


Figure 3. Uncinate Fasciculus in its Euclidean Space

water molecules that participants have into the central nervous system. Result of that meeting is a NIFTII data format that can be extracted to form the matrices concatenated chain. The dimensions of the FOV are not equivalent to the dimensions of the native brain space, since the brain does not have a defined rectangular topology. It is a factor in the acquisition to place a FOV that includes the cerebral parenchyma-cerebellum, at the same time has the least amount of NaN. However, post- processing allows cropping, which adjust the FOV and the brain to reduce NaN percentage.

The system to assign coordinates to minimal units can be observed in the example of the (Figure 4), the uncinate fascicle is traversed by JACtree through a scanning system that systematically assigns an arbitrary scalar, in our case 0 (zero) to the extreme left higher back wall of the Euclidean space, maximum scalar is assigned to the end point located at the opposite extreme of the same Euclidean space. The three vectors (color codified by FEFA international standard) contain a Uncinate Fasciculus (UF), represented in blue dots. Distance to Centroid Median allow to distribute the points of information containing information concatenating FA|MD to radial/transversal position.

The blue dots that represent the UF have a unique scalar identification. In the following figure (Figure 5) part of the FOV matrix show NaN and connectivity points of information values.

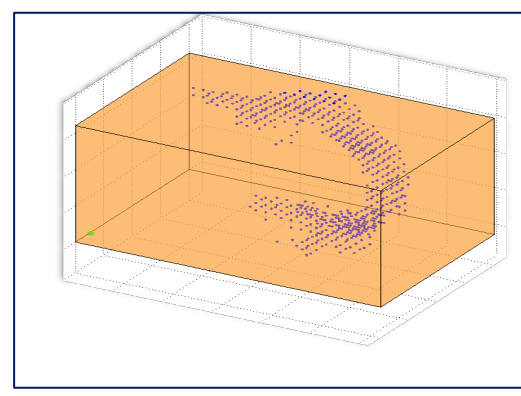
An algorithm that JACtree implemented makes a sweeping operation under rise and curvature rules that assign scalar to each minimal point in a systematic way of acquisition/extraction) to each coordinate. Regarding the Euclidean distances of each point of information (voxel based) in the Euclidean space that contain the WMT in analysis. To reach that topology does an along streamline analysis, which means to build a $[m \times n]$ matrix representing the WMT. To get that matrix uses the voxel information as points of information. JACtree proceeding resample the WMT extracted using Boolean operators in a matrix platform [24,25]. Each tract has x points (e.g., x voxels), then point 1...i form bandwidth axis X, axis Y, axis. (Figure 1) illustrates the result of that combination process (Figure 6).

Points of information are distributed on X,Y,Z orthogonal vectors combination. A transversal cut defines positions respect a centroid. The centroid is a result of $[X,Y,Z]$ Median at each advancing point of the streamline. Then, points of information belong to a streamline but have a particular distance to centroid depending on the resulting equilibrium distance of $[X,Y,Z]$ Median values. A consequence is that in the same streamline the points of information can change the position enough to pass to another ring in a cross-sectional point. The topology of WMT

is orthotopically forced by vectors that exert deformations, captured by wave signals in ageing [17]. Relevant is to bear in mind the warning about the difference between the quality of the images and the poor results provided by DTI for understanding the relationship between structural connectivity and cognition. The correlation coefficients show low levels; the articles are characterized by a low number of cases, a poor base of physical and mathematical knowledge, lack of recognition of technical impossibilities to detect fascicles that are reported as WMTs in research, and exaggerated statements such as “found solid evidence” where relationships between the tracts connectivity and cognitive processes try to link tasks of difficult intelligibility. This is why the title “Just pretty pictures” [26] has its sense. Fishing papers characterizes by listing more than one hundred of behavioral variables, a set of brain structural connectivity data without theoretical guide, a uniaxial concept of WMTs material [14-17]. The following figure shows the ventral Uncinate Fasciculus, circled in red. At right a subset of a large list of matrices exhibit what is determining the ‘nice pictures to show’. The quality of visual presentation is an aesthetic performance solidly based on rigorous principles of imaging science physics, software (e.g, ExploreDTI) is widely recognized [24].

The following figure show the JACtree plot of the same information. It is clear that data was affected by Procrustean mathematics, because the matrix is fulfilled with points of information (Figure 7):

The figure above also shows that a concatenated set of matrices convert a brain native space in a set of nested-hierarchical information. One of the matrix's save the size of the Euclidean space of whole brain tractography, an array vector with only three values. But this simple algebra initiates a chain of information melody in order to extract a WMT where is necessary to apply Boolean logic. Then a WMT is also a Euclidean space (complex set theory). To return to JACtree, the pipeline brings a subset of the points with information that represent a WMT in approximately 5-10% of the (A A1) informative Euclidean space. To explore the radial dimension of a WMT JACtree strategically face the streamlines bandwidth and longitude considering both dimensions correspond to different kind of variables, a) bandwidth is an ordinal variable where streamlines are positioned in A= $[m \times n]$ matrix b) longitude is fulfilled applying points of diffusion tensor information, the original MR readout. To highlight the methodology, crucial is to



92x73x65; 6,43%-NaN

Figure 4. Uncinate Fasciculus represented by the blue dots. Euclidean space dimensions were printed in the standardized color code

92x73x65 double									
0.1418	0.3357	0.4059	0.3436	0.3793	0.4805	0.3912	0.2471	0.3046	
0.1660	0.1915	0.1590	0.2661	0.4176	0.3843	0.2537	0.1444	0.1369	
0.1196	0.1059	0.1503	0.2364	0.4417	0.3790	0.1997	0.1004	0.0789	
0.1624	0.1862	0.1367	0.1893	0.4603	0.4091	0.1655	0.1082	0.0862	
0.2739	0.0775	0.0795	0.2034	0.3767	0.3010	0.0929	0.0611	0.0925	
NaN	0.1811	0.2088	0.3055	0.3148	0.2036	0.1058	0.0415	0.0833	
NaN	NaN	0.2291	0.3181	0.2427	0.1137	0.0760	0.0748	0.0516	
NaN	NaN	0.0734	0.1452	0.1543	0.0830	0.1030	0.0848	0.0657	
NaN	NaN	0.0698	0.0695	0.0836	0.0454	0.0593	0.0820	0.1010	
NaN	NaN	NaN	0.0892	0.0741	0.0753	0.0873	0.1097	0.1305	
NaN	NaN	NaN	0.1568	0.1146	0.0917	0.1347	0.1238	0.1039	
NaN	NaN	NaN	NaN	0.2104	0.1028	0.0975	0.1148	0.0962	
NaN	NaN	NaN	NaN	0.2439	0.1064	0.0595	0.0766	0.0876	
NaN	NaN	NaN	NaN	NaN	0.1296	0.0529	0.0636	0.0908	
NaN	NaN	NaN	NaN	NaN	0.1683	0.0467	0.0985	0.1557	
NaN	NaN	NaN	NaN	NaN	NaN	NaN	NaN	NaN	

Figure 5. Up-Left is detailed the size of the Uncinate

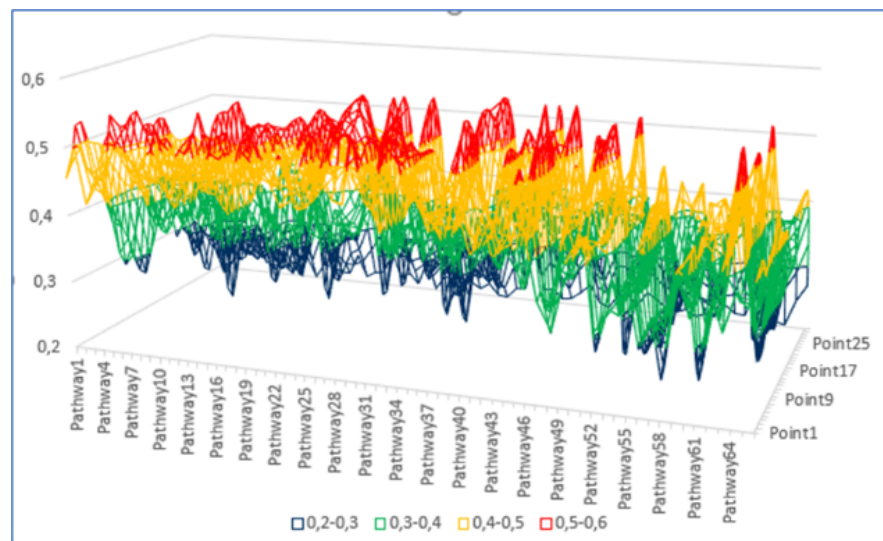


Figure 6. Fractional Anisotropy (FA) by pathway (streamline-longitude) and bandwidth of the white matter tract

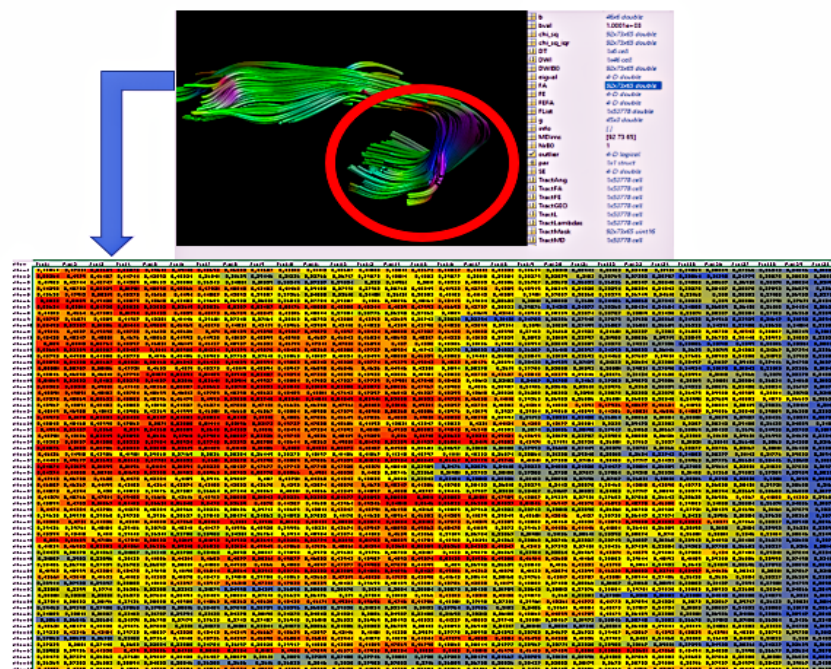


Figure 7. Matrix of a Ventral Uncinate Fasciculus. Hot colors represent higher Fractional Anisotropy. The blue in the right belong to the Uncinate steam

change the central tendency representative measure. For the bandwidth is necessary to calculate the Median, considering the three axes forming each point in a transversal mode, as was mentioned before. The centroid of the tree Medians allows to calculate the centroid of the WMT at point(x), that not necessary correspond to an informative point of the Euclidean subset space. If the WMT has 76 large minimal measure (e.g., voxels), similar N= 76 centroids will be calculated using the 'Median 3-D cross'.

In topology terminology, the tubular form of WMTs is similar to an ellipsoid. Each streamline has a distance to the centroid = Euclidean². JACtree adapting to the orthotopic-eccentric material of WMTs, proceeds statistically to the mentioned correspondent variable class: a) ordinal and b) interval variables, for a) width (3-D) to b) large (informative minimal points). Median and Mean are applied, being conscious that FA is a fractional expression (not a ratio/interval variable *strictum sense*). Wrongly was treated as a proportional variable [19,27,28], exposing 'reference data' (proposing a dataset as a reference scale, [27]). The fractional expression FA can be understood as a) organization divided by b) disposable to organize quantum. A common error is to confound mean diffusion with the denominator of the FA formula. Mean Diffusion represent a pre-organized quantum, differentiating to the Apparent Diffusion Coefficient (ADC) [29].

JACtree obtain the necessary m*n matrix treating the longitude of the WMT with along tract analysis [25] but modified to reach an along streamline analysis. Mathematics of Procrustean [30] average the longitude, throwing a Procrustean effect coefficient (is recommended not overpass 0,05 impact). JACtree report the effect of Procrustean, results to obtain a m*n matrix after Procrustean mathematics in a Euclidean Space report values lower than 0,001. (Figure 8) compare two UF a) without along streamline analysis b) the same tract applying Procrustean JACtree:

The dynamics of extension-contraction of the streamlines use the minimal diffusion tensor points-voxel based, as points of diffusion tensor information. Regarding the Euclidean space, giving a 3-D matrix with FA|MD information, then a sizeable m*n matrix initiates the way to use the centroid as a gravity center to form rings surrounding that topology.

The [A] Matrix has distance to centroid values, [B] matrix inform the orientation and distance to centroid, [C] matrix Fractional Anisotropy values for each point, [D] matrix correspondent Mean Diffusion. As [A B C D] have similar dimensions, all linear algebra operations can be done. The three-dimensional structure of the tract is saved in a chain.

[A matrix, B matrix positions by point, C and D structural connectivity information]

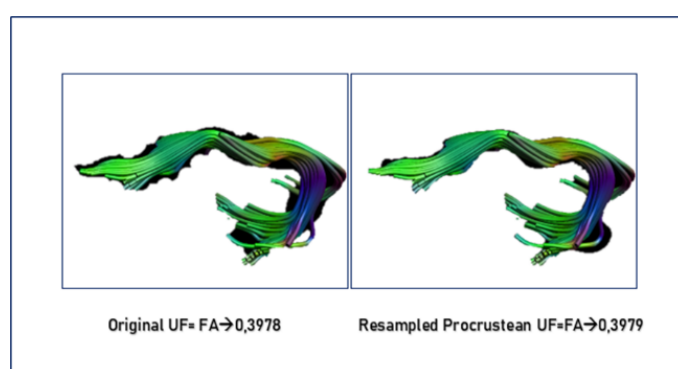


Figure 8. The same Uncinate Fasciculus treated with and without Procrustean JACtree. Fractional Anisotropy results are reported

Part B

Introduction to the Uncinate Fasciculus

All subsamples will be analyzed focused on UF. This strategy is directed to probe the consistency of JACtree results, specially the analysis of the radial microstructure. The Uncinate Fasciculus (UF) is a White Matter Tract (WMT) characterized by a sickle shape. It has a flattened dorsal part that enters the orbitofrontal part and the inferior prefrontal gyrus. Then a stem crosses the anterior temporal region and begins the ventral part. This part communicates with the limbic system, the ventral fibers-UF enter the amygdala and different parts of the insula. The division of the UF into three parts is characteristic of the literature, however we applied JACtree. The three samples we will present anticipate UF has this organization: Central DorsalUF (cdUF), External DorsalUF (edUF), Central VentralUF (cvUF) and External VentralUF (evUF). The stem had an insignificant proportion of fibers, stretched in the curve that temporal lobe and prefrontal lobe form in its union. Its fibers were attributed to ventral UF. The resultant model of UF (Left-Right) is sketched below. Our previous data support findings and antecedents that assume a subcortical interhemispheric connection via *terminalis stream*. These results were published in a design that related the volume of the Orbitofrontal Cortex and the connectivity of the UF. It was a combinatorial study of Voxel-Based Morphometry and Diffusion Tensor Images. The recent report of Nomi, *et al.* [31] reinforce that hypothetical ground. UF was related to Emotional Regulation (ER), Language Network (LN) and Appraisal [32-36]. ER is a set of mechanisms to diminish, amplify, suppress the emotional impacts [37]. There are a) spontaneous individual ER subsets, e.g., to take a walk in the street after a discussion in a couple b) instrumental ER subsets implemented in therapeutical contexts and/or reported in experiments, like reappraisal [37-39]. Interestingly, reappraisal represents a complex use of cognitive capacities to reframe an emotion, mainly a negative one. The work of Kalisch, *et al.* [40] showed that reappraisal implies working memory, conceptual tracking [33], executive functions. It is highlighted because ventral UF is considered linked to appraisal, dorsal UF is related to the language processing of the appraisals. In a combat metaphor, the ventral UF would be located at the first line, dorsal UF would be the strategical center that is not in the field of the battle. A model of UF system helps to organize the following section (Figure 9):

Experiment 1

Sample

The sample was composed of 34 Argentinian healthy volunteers aged between 20 and 38 years ($M = 25.91$, $SD = 4.98$), of high education level, of which 21 were women. The study protocol was accepted by the Oulton Ethical Committee in accordance with the principles of the Declaration of Helsinki and the participants provided informed consent for their participation in the study.

Procedure

We applied a task previously adapted by our group to measure semantic control manipulating strength of association and semantic-affective congruence between words (for a recent example, please see [10]). Participants were presented with cue words and were asked to choose the most closely related meaning among three options. Items varied in the strength of association between the cue and target. Weak associations have been shown to activate the semantic control network, along with other task manipulations such as ambiguity and strength of distractors.

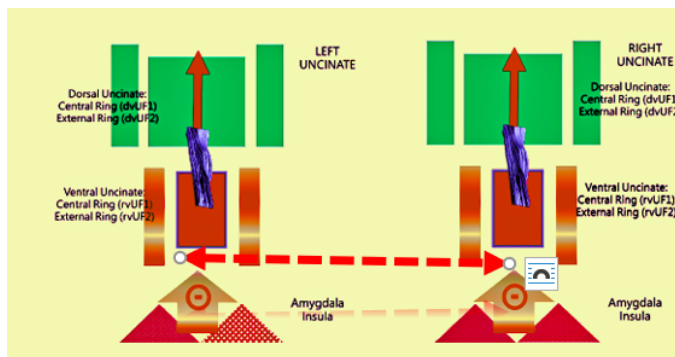


Figure 9. Model of Uncinate Fasciculus System

Marino also added a manipulation of semantic-affective congruence: the semantically related options were either congruent in terms of valence (i.e., both positive or both negative) or they were incongruent (one word was positive and the other was negative). In this previous study, there was a bigger effect of congruence for weakly-associated items, suggesting that when controlled semantic retrieval demands are already high, a mismatch in the emotional connotation of words increases control demands further. The words were rated for their affect, control, and arousal, in order to generate semantic-emotional conflicts. The task contained 192 items, with 64 items that were affectively congruent, affectively incongruent, and neutral (no affect).

MRI acquisition

All participants were informed of the precautions required for MRI acquisitions. After entering the scanner, five minutes of relaxation and adaptation were given to all participants. The complete MRI acquisition that followed had duration of 22 minutes.

Images were acquired on a Philips Achieva 1.5 T scanner, using a 12 element SENSE head coil. Thirty-two diffusion weighted and one non diffusion-weighted volume were acquired by eco-planar single-shot imaging, with the following parameters: b -value = 1000 s/mm², TR/TE = 9900/80 ms, acquisition and reconstruction matrix size = 112 x 110, FOV = 22.4 x 22 cm, slice thickness = 2 mm, number of slices = 60. In order to correct the DWI for EPI distortions, a structural T1 image was acquired with the following parameters: acquisition and reconstruction matrix size = 240 x 240, TR/TE = 7.05/3.24 ms, FOV = 25.6 x 25.6 cm, number of slices = 249, slice thickness = 1.1 mm, flip angle = 8°.

Image processing

The MR images were processed using MATLAB R2014a and ExploreDTI 4.8.6 [25]. First, Gibbs ringing artifacts in the b0 images were corrected with the total variation method. Then, subject motion and eddy current induced artifacts were corrected by applying an affine registration of the DWI to the b0 image. The b-matrix was accordingly rotated [23]. The DWI were non-rigidly registered to the T1 image to correct for distortions due to echo-planar imaging. Finally, the FACT algorithm was used to perform whole-brain DTI-based deterministic tractography, with the following parameters: fractional anisotropy threshold for streamline initiation and continuation = 0.2, length threshold 10-500 mm, step size = [2 2 2] mm, angle threshold = 35°.

DWI analysis

A semi-automated tractography dissection method was applied, previously presented in Lebel, Walker, Leemans, Phillips, & Beaulieu [27]. In short, this method requires drawing regions of interest in a reference space to obtain the tracts of interest. The reference space is

then registered to the subject's space, and the regions of interest are adapted to obtain the tracts of interest for each subject. In this study, the reference space was an individual case randomly selected from the sample. The methodology for *in-vivo* tractographical dissection by region of interest drawing is thoroughly described.

Results of Experiment 1

JACtree statistics

Contractio descriptive and inferential (Table 1, Figure 10):

Experiment 2

Sample

The sample was composed of 161 healthy volunteers aged between 18 and 31 years (M=20.28, SD=2.47), of which 64 were men. These volunteers were students from the York University, Yorkshire, UK, and provided informed consent. Given this is a reanalysis, for further details please refer to the data in the original paper of Davey.

MRI acquisition

Diffusion weighted MRI data was collected using a 2D single-shot pulsed gradient spin-echo EPI sequence (TR = 15,000 ms, TE = 86 ms, matrix = 96 x 96, 59 slices, voxel size = 2 x 2 x 2 mm³; b = 1000 s/mm², 45 diffusion directions, 7 B0 volumes, 13 min).

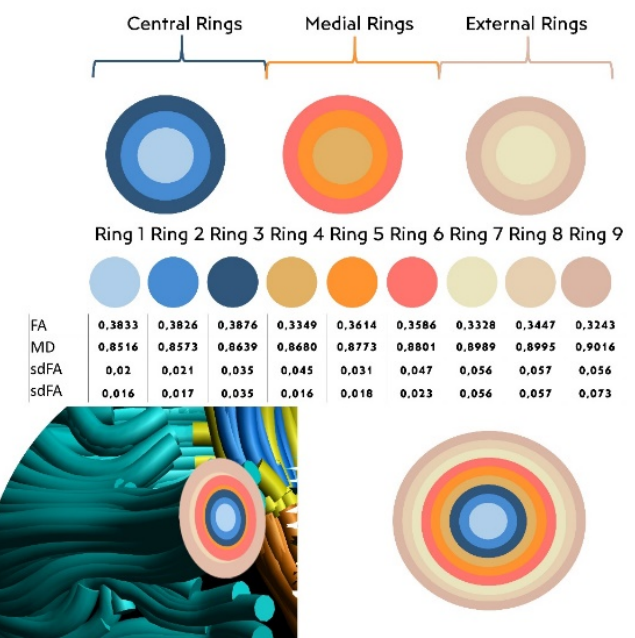


Figure 10. Contractio JACtree report: Null hypothesis WMT in analysis is uniaxial *mnc* material: Rejected. Orthotropic-Radial organization suggested: Concentric. Cluster analysis: 2 clusters (Euclidean Distance²)

Table 1. JACtree statistics. Output of the software including figure and table

Uncinate Fasciculus (complete)
Fractional Anisotropy Mean (sd): 0,356 (0,239)
Mean Diffusion (sd): 0,857 (0,018)
FA Change Ratio: 53%
MD Change Ratio: 51%
Moment-Product Coefficient (concentricity*FA): $Q=0,924$, $p < 0,001$
Moment-Product Coefficient (-concentricity*MD): $Q=0,928$, $p < 0,001$

Image processing

The MR images were processed using MATLAB R2014a and ExploreDTI 4.8.6 [25]. First, Gibbs ringing artifacts in the b0 images were corrected with the total variation method (Table 11). Then, subject motion and eddy current induced artifacts were corrected by applying an affine registration of the DWI to the b0 image. The b-matrix was accordingly rotated [23]. The DWI were non-rigidly registered to the T1 image to correct for distortions due to echo-planar imaging (Table 12). Finally, the FACT algorithm was used to perform whole-brain DTI-based deterministic tractography, with the following parameters: fractional anisotropy threshold for streamline initiation and continuation = 0.2, length threshold 10-500 mm, step size = [2 2 2] mm, angle threshold = 35°.

DWI analysis

A semi-automated tractography dissection method was applied, previously presented in Lebel, Walker, Leemans, Phillips, & Beaulieu [27]. In short, this method requires drawing regions of interest in a reference space to obtain the tracts of interest. The reference space is then registered to the subject's space, and the regions of interest are adapted to obtain the tracts of interest for each subject. In this study, the reference space was an individual case randomly selected from the sample. The methodology for *in-vivo* tractographical dissection by region of interest drawing is thoroughly described in Wakana.

Behavioral measures

Instruments: Different scales and self-reported inventories were applied in the NS-1 cohort of the Center for Neuroimaging at the University of York. The instruments were applied by researchers from the Department of Psychology, led by the author of this work E.J. Instruments that had questions about mood, emotions, as well as personality and anxiety inventories were used. As the tasks were applied by other researchers, the details are found in the open publications in the reservoir of the University of York, UK.

An important aspect is that self-reported inventories have the bias that the magnitude depends on the magnitude intelligence of the participants. For example, in a previous study we detected that there are personality traits linked to extraversion associated with placing higher scores on all scales. This should be interpreted as follows: When an instrument has several factors, the magnitude of each factor per participant must be interpreted inter-related with the remaining factors. The absolute value should not be considered, because the participants have consistent differences between different tests in the quantities by which they score the items (Figure 13).

A practical example of the above is the following: A participant who has the highest Neuroticism score on the MMPI Personality Inventory, had the proportionally highest Agreeableness score. When looking at her score on the ERQ, she also had the highest scores on suppression, but they were the highest in the entire sample at Reappraisal. Therefore, her intelligence of magnitudes leads her to consider that what happens to her is always very high. On the other hand, there are participants who relativize her situation with respect to other people, and place average scores, since they interpret that the magnitude of it is not extreme before what happens between people. Hence, the inventories that measure factors are interpreted in terms of proportions to each other.

Results

JACtree report of orthotropic-radial structure using CONTRACTIO. The Table is included to illustrate the software reports (Table 2):

JACtree cluster report of rings (Figure 14). The dendrogram classified again two rings, ranging one to five and six to nine (see Figure 15).

In order of the cluster results UF system was organized in the same way than experiment one. Correlations were performed between UF-Left, Right-Dorsal, Ventral-Central, External* a) MMPI-proportional data reading b) Trait Rumination of Multifactorial Assessment of Interoceptive Awareness (MAIA) c) Describing a Friend (DAF) content analysis c1) proportion of self-references c2) proportion of behavioral narrative d) Trait Anxiety of STAI e) Social Anxiety Scale extracted of WHO well-being scale. UF Uniaxial FA|MD was also included, The following Figure-Table has the original software report. It can be appreciated a new distribution of color rings, corresponding to clustering. Also, the microstructure values of each ring, averaging the sample (Figure 16):

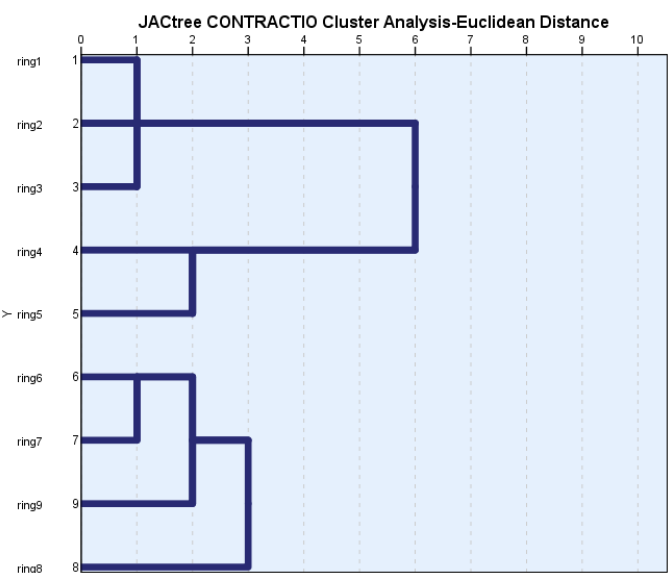


Figure 11. JACtree Cluster Analysis CONTRACTIO: Cluster 1 (r1-r5); Cluster 2 (r6-r9)

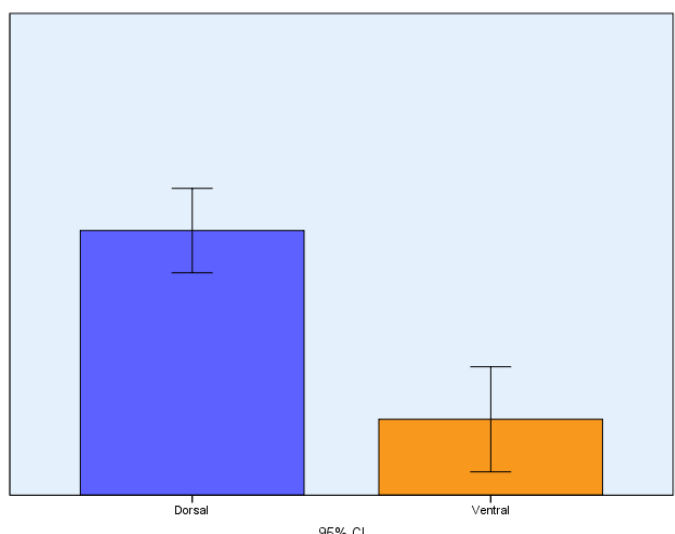


Figure 12. Longitudinal Analysis: Dorsal versus Ventral Uncinate Fasciculus

Experiment 3

Sample

The present study re-analyzes the cases presented in Reynolds, *et al.* [13], where magnetic resonance imaging (MRI) and behavioral data was collected from a sample of 181 children from the city of Calgary (Canada), with the application of an innovative technique that does not require infants to be sedated [11] during acquisition. It

Table 2. JACtree Contractio report

JACtree CONTRACTIO Report	
FA White Matter change %	52%
FA Rate of Change	37%
MD White Matter Change %	59%
MD Rate of Change	18%
FA Moment-Product Coefficient	0.91 concentric order
MD Moment-Product Coefficient	0.78 concentric order
FA Moment-Product Coefficient Null Hypothesis	-0.05 Uniaxial rejected
MD Moment-Product Coefficient Null Hypothesis	-0.03 Uniaxial rejected

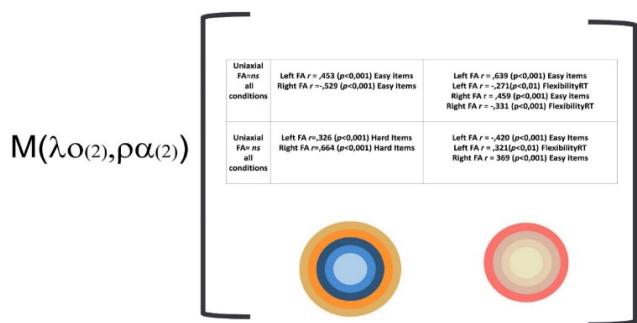


Figure 13. Correlation matrix comparing uniaxial mnc versus Orthotropical- Radial approach, together with clustered rings

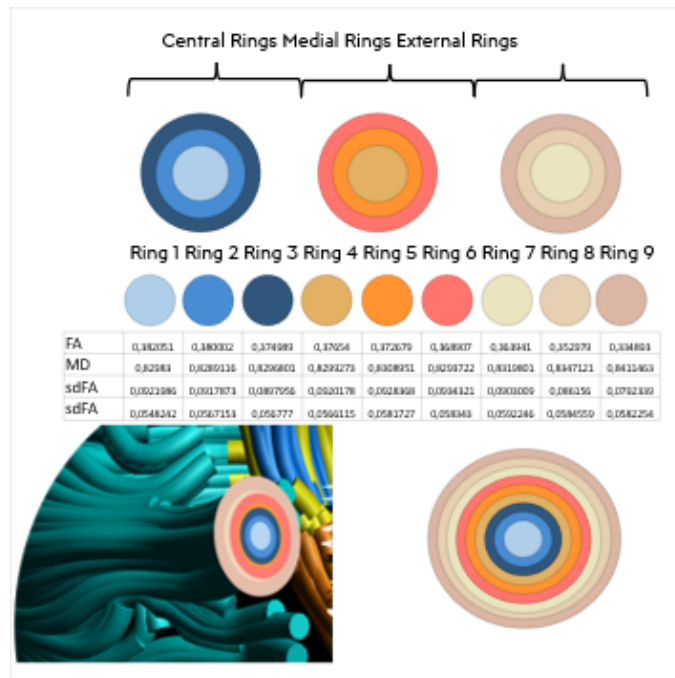


Figure 14. Output as JACtree report statistics of CONCENTRIC tool

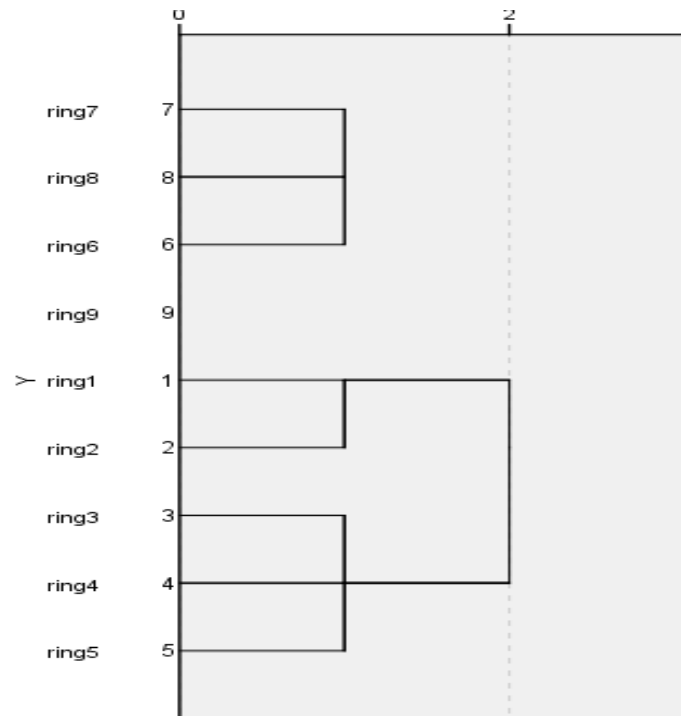


Figure 15. Cluster analysis of rings as reported by JACtree

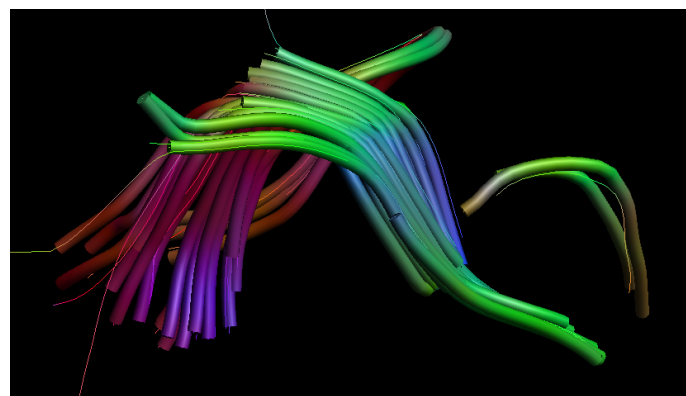


Figure 16. Output as JACtree report statistics of correlation matrix and extracted rings

was a population aged 3 to 5 years ($M=4.067$, $SD=.569$), constituted of 86 girls and 95 boys. As reported, all children were born at full term (>37 weeks' gestation), were free from diagnosed neurocognitive or developmental disorders, spoke English as a primary language, had not yet received any formal reading instruction, and had not reported any contraindications to MRI scanning. Some of them were scanned 2, 3 and 4 times. In this work we will work dividing the sample every 6 months. In this way, the change in the evolution of Uncinate Fasciculus can be observed.

Procedure

All imaging was conducted by the Developmental Neuroimaging Lab at the University of Calgary (<https://www.developmentalneuroimaginglab.ca>) using the same General Electric 3T MR750w system and a 32-channel head coil (GE, Waukesha, WI) at the Alberta Children's Hospital in Calgary, Canada. Children were scanned without sedation, either while they were awake and watching a movie of their choice, or while they were sleeping. In addition to the

acquisition of magnetic resonance imaging, on the same day the infants were evaluated on their pre-reading skills, applying the phonological awareness and naming NEPSY-II subtests.

MRIacquisition

T1-weighted images, ASL, diffusion-weighted (DW), and passive viewing fMRI data were acquired as part of a longer MRI protocol (~45 minutes total). DW-MRI images were acquired using a single-shot spin-echo echo-planar sequence with the following parameters: TR=6750 ms, TE=79 ms, resampled voxel size (in post-processing) = $2.2 \times 2.2 \times 2.2 \text{ mm}^3$; b=750 s / mm², 30 diffusion directions, 5 B0 volumes, field of view = 20.0, duration = 4:03 min.

Image processing

It is important to note that the processing pipeline was executed by our group. The acquired DW-MRI were processed using MATLAB R2014a, ExploreDTI 4.8.6 [25] and JACtree 7.0. First, the Gibbs ring artifact in the B0 images was corrected with the total variation method. Movement correction and eddy current artifact correction were performed on the subject's native brain space [23]. A whole brain tractography was generated on the reconstructed matrix using the FACT algorithm, excluding fibers with a length of less than 10 mm and greater than 500 mm; an AF range between 0.20 and 1 was established, and a 'linear' interpolation method was used.

DWI analysis

A semi-automated dissection method was used, originally presented in Lebel, *et al.* [27]. This method requires defining regions of interest in a reference space to obtain the tracts of interest. Then the reference space is registered to the native space of the cases, and the regions of interest are adapted to capture the tracts in each subject. In this study, the chosen reference space was that of an individual selected from the sample. The methodology for in-vivo dissection of tractography by regions of interest has been described in detail in Wakana.

Results

Group 1 (3-3.5 age)

Only the development of the dorsal part of the UF can be observed. The area corresponding to the stem that will join the ventral and dorsal parts is located in the dorsal part. There is no entry of the UF into the subcortical space (Figure 17).

Group 2 (3,5-4 age)

The incipient development of the ventral part is observed. The difference in size between the dorsal and ventral part is equivalent to 300% in favor of the first. The orthotropic-radial structure is as follows (Table 3, Figure 18):

Group 3 (4-4,5 age)

At this age it is observed that the Mean Diffusion starts its growth rate, while the Fractional Anisotropy has not yet developed. The volume changes substantially, the ventral part begins to grow (Table 4, Figure 19).

Group 4 (4,5-5 age)

At this age, a pattern is observed that will later be repeated in the adult: A growth rate of AF with a lower rate of change in MD. It is interesting that the beginning of the adult configuration can be seen a) A high rate of MD especially in the outer rings, but with a small

Table 3. JACtree Contractio report

JACtree CONTRACTIO report		
FA White Matter change %	57%	
FA Rate of Change	72%	
MD White Matter Change %	112%	
MD Rate of Change	50%	
FA Moment-Product Coefficient	0,49	concentric order
MD Moment-Product Coefficient	0,82	concentric order
FA Moment-Product Coefficient Null Hypothesis	-0,10	uniaxial
MD Moment-Product Coefficient Null Hypothesis	0,09	uniaxial

Table 4. JACtree Contractio report

JACtree CONTRACTIO report		
FA White Matter change %	17%	
FA Rate of Change	ns	
MD White Matter Change %	70%	
MD Rate of Change	21%	
FA Moment-Product Coefficient	0,08	concentric order
MD Moment-Product Coefficient	0,55*	concentric order
FA Moment-Product Coefficient Null Hypothesis	0,00	uniaxial
MD Moment-Product Coefficient Null Hypothesis	-0,01	uniaxial

Table 5. JACtree Contractio report

JACtree CONTRACTIO report		
FA White Matter change %	53%	
FA Rate of Change	78%	
MD White Matter Change %	77%	
MD Rate of Change	16%	
FA Moment-Product Coefficient	0,44*	concentric order
MD Moment-Product Coefficient	0,29*	concentric order
FA Moment-Product Coefficient Null Hypothesis	-0,04	uniaxial
MD Moment-Product Coefficient Null Hypothesis	0,00	uniaxial

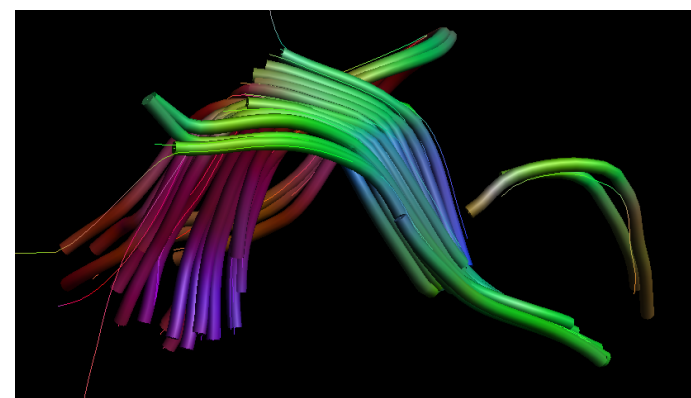


Figure 17. Uncinate Fasciculus at 3,2 age

standard deviation b) A jump in the joint growth of FA and MD from the middle rings c) A stopping of the MD in ring 4, with an increase in the FA in ring 3. In the central ring the FA stops, but the MD decreases significantly. That is the adult pattern, an interaction between FA and MD that can be summarized in three stages (Table 5, Figure 20).

Dorsal to Ventral comparison was not possible because at this age the Ventral UF is not developed to have enough streamlines. But was possible to analyze the FA|MD relation of dorsal UF. To perform this analysis, JACtree *lja* (*lja*) tool was applied. *Lja*-JACtree analyze the progressive relation between MD|FA in a linear relation, while *logch* analyze the logarithmic relation between FA|MD. This tool allows to examine in detail the FA|MD relation. Above the three rings of Children

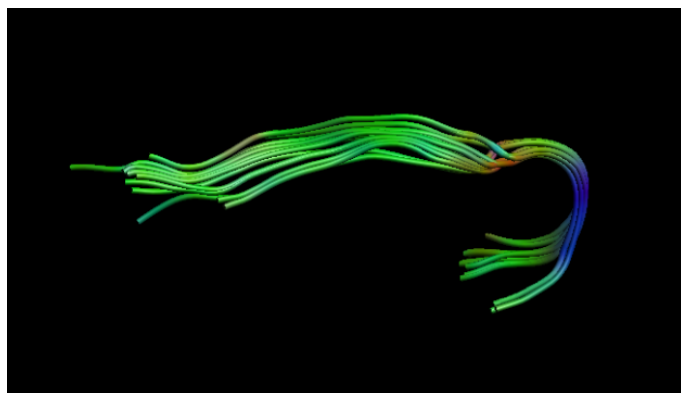


Figure 18. Uncinate Fasciculus at 3,9 age

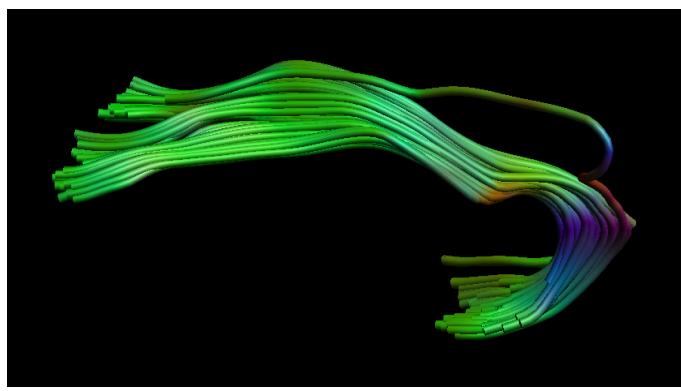


Figure 19. Uncinate Fasciculus at 4,2 age

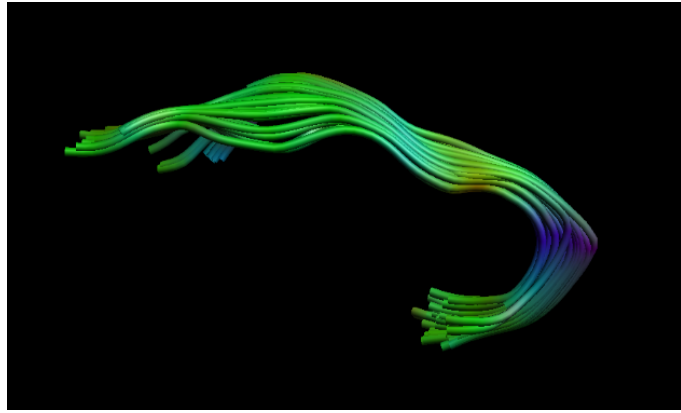


Figure 20. Uncinate Fasciculus at 4,8 age

Contractio illustrate how at 4,5-5 age the FA|MD relation is near to an adult one (Figure 21).

The fractional expressions FA/MD considering each ring were the followings (Table 6):

Then we add the use of standard deviations, the effect that the off-diagonal elements of the diffusion tensor have when orthogonal rotation is performed to produce the diffusion ellipsoid. This implies that tool, analyze how the variance not included in the eigenvectors (L1, L2, L3) is included by the tractography algorithm in the module that forms the eigenvalue of L1, L2, L3. This implies an additional article, but it is illustrated that JACtree statistics basics relay to know the relationship between FA | MD. It is recalled that the origin of JACtree lay in the inconsistencies about the opposition that the texts present between FA |

MD, since both are constructed with the same eigenvectors. At the same time, different associated constructs are attributed to FA | MD, which motivated an analysis inside the algorithm statistics to know the effect of multiple regressions and factorial solutions through orthogonal rotations. These statistical skills are necessary, but it is important to know that they are skills of that nature, because the data stored by the readout matrices are treated according to a mathematical model that produces representations of tracts. In this case, the model is a DTI one. Results presented in an article are an effect of these manipulations, newly, necessary to generate a whole brain tractography. Also, necessary to know that, because other models, as Diffusion Kurtosis Imaging (DKI) appear as technological progress. They are related in a significant proportion to that, but it is not the essence of DKI/DTI differences. Mathematical proceedings have a proportion of explanation, also.

Discussion

This study presented an orthotropic-radial approach to DD-MR. It arose from two sources: a) the controversy about what FA | MD measures b) the relatively poor results provided by structural brain connectivity and cognitive and affective processes. On point a), by performing scatterplots that related MD (x-ax) and FA (y-ax) in Cartesian coordinates, it was observed that a point-by-point WMT has a bandwidth and a length; the bandwidth x length points showed regularities. There were streamline without labels whose length points remained at the e.g., N = 131 length points of the Lower Longitudinal Fasciculus, higher in FA and lower in MD. By drawing a Latin square, three phenomena could be observed: 1) stable longitude perceptions of streamline points with high FA 2) perception of longitude points 'pivots' 3) perception of longitude points of streamlines with low FA. This alerted the possibility of an organization in the streamlines, for which it was necessary to know its location within the set of streamlines of the WMT. For example, the adult ILF reaches a bandwidth of 120 streamlines to 150. However, how to know where they were located

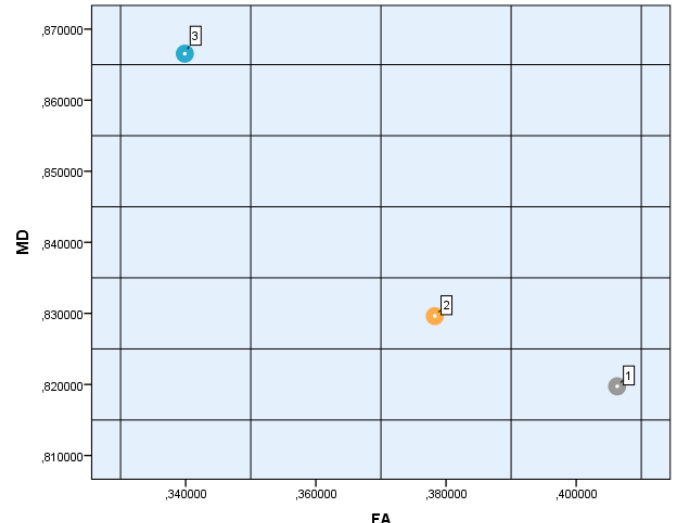


Figure 21. JACtree CONTRACTIO for children (three rings)

Table 6. linear and logarithmic relation between FA/MD by rings

Ring	linja	logch
1	0,495634926	1,786973364
2	0,455964966	1,89249471
3	0,392211336	2,119039825

if they were not labeled? On three dimensions, a number could be misleading, because 234567 could be located in the right hemisphere, and 234568 in the opposite. The scatterplots indicated configuration of perceptions, clouds that move, point to point, within storms. We called storms to points where all dots were regularly linear organized. The following points return to the cloudy organization.

For this, a method of assigning a scalar to each streamline, regardless of the point of longitude, was designed. The method arose from the algebra of matrices, if each brain native space is in a Euclidean space, then it is a rectangular cube. Therefore, if a 0 was defined at one extreme, choosing the highest extreme, from the left and occipital, its opposite had to be the maximum number. So, if the Euclidean matrix of a tract has three dimensions, the text mentions $76 \times 91 \times 80$, doing the multiplication gives the number of points. In this way, you had to assign a 0 to that position and the result of the multiplication, 553280.

In the Euclidean space of the uncinate fascicle that is below the points that correspond to the WMT are observed, also empty spaces. Through an allocation system, which was starting from 0 towards the front, when reaching the top, returning to the neighboring occipital spine, when it reached a corner and descended, it maintained the criterion of starting from the left, highest point, occipital, then all the streamlines had a numeric label (Figure 22).

The passage from perception of regularities to numerical labels was the discovery. The clouds that remained at the top of FA had the same scalar (the source value of the streamline). Then the peculiarity arose that the values that formed the clouds had scalars such as [4 5 6 7 8 13 14 15 16 20 21 22 23 24 25 31 32 33 34]. That was a typical pattern, adjacent numbers jumping to another cluster of adjacent numbers. When comparing the scalars of origin of the bandwidth with the regularities, it appeared before our eyes that they were organized in a radial way, with concentric circles. Furthermore, the highest FA values occupied the center of the Euclidean space, thus the idea that there was a transversal organization arose. Up to 17 tests were carried out in different WMTs, and the same thing happened in all. The organization had three stages that were repeated: 1) in the FA | MD relationship, the high FA value could or could not be related to high MD 2) the outer circles had high MD, approximately in the middle of the radius the FA rose significantly, from immediately, the growth of the MD stopped, and a growth of FA began, 3) until the central point the value of MD was low and the value of FA, proportionally, was the highest.

Consulted Beaulieu (personal communication), indicated that it could be a Partial Volume Effect. Consulted Leemans (personal communication) suggested generating a high number of rings and contracting them progressively. In this way, according to what Vos, *et al.* [21] proposed about the PVE, if the effects were maintained they had total independence from the influence of partial volumes, since the Contractio tool emerged in that way, making the connectivity values independent with rings independent. The number of $N = 9$ rings was sufficient, since the WMTs combined FA | MD so that two or three rings were explanatory, but the contraction had to serve as the null hypothesis (Figure 23).

The nine colors of Contractio indicate three rings subdivided into three. Using RGB code, the outer rings have khaki, Navajo white and burlywood colors, taken from photographs of landscapes of southern Patagonia, so that the lumen is the same. The central colors are coral, salmon and darkorange, while the center has the different colors of the sea: steel blue, cadet blue and sky blue. Contractio was a test, but the WMTs are organized, with the readout system and the mathematical

model used, in two or three rings, according to the cluster analysis based on the squared Euclidean distances of each point of equivalent information in the “green” axis of the FEFA color code, in relation to the centroid. The centroid is obtained from the entering medians of the three dimensions that intervene at each point of length advance. This explains why the same streamline can have length points in one ring and then in another, to return to the previous one (Figure 24).

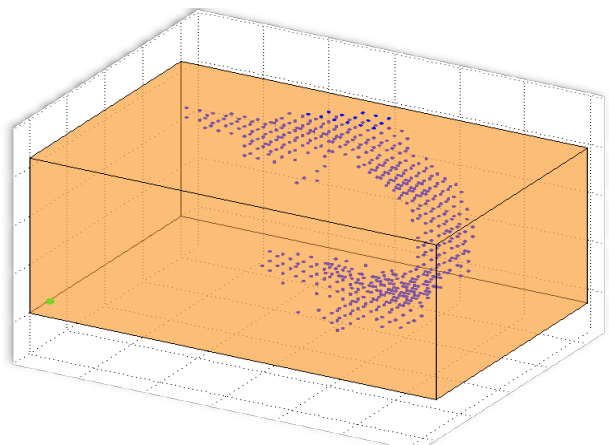


Figure 22. JACtree point plot of uncinate fasciculus

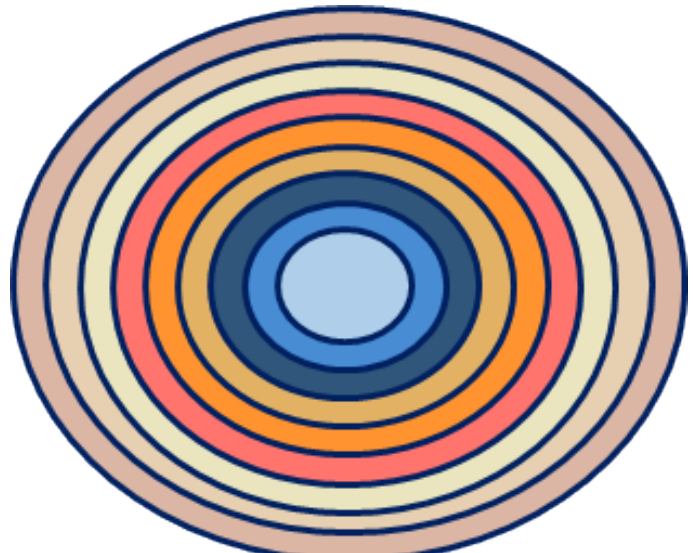


Figure 23. Radial rings color-convention of the JACtree software

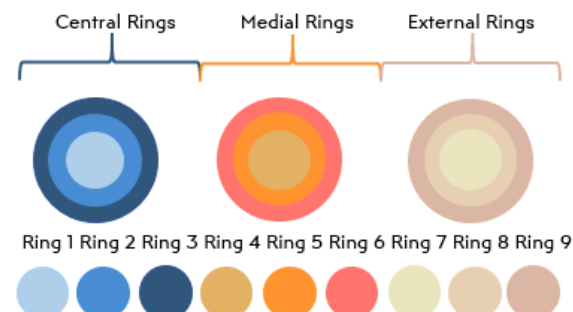


Figure 24. Radial ring colors by centrality-extensality

The findings had a robustness and stability that a background check was used. There were indirect antecedents, such as Balo's Multiple Sclerosis, which proposes that WMTs implode by different levels of tension within them. MR elastography work is rare, but reports indicate that WMTs are orthotropic material, meaning that it receives force vectors. Due to its flexibility, it can resist, but the passage of time showed evidence of loss of the one signal when a sound [17] was applied to the radiated crown. In materials physics, the literature classifies materials that are flexible and different forces dispute their shape, or uniaxial materials, such as steel. Clearly, a biological device like WMTs had to have orthotropic properties. This type of material is not only a pipe but also a creator of algorithms to support cognitive and affective processes. This aspect was crucial, since the studies with mathematical models DTI, DKI, are formed by physicists who are unaware of these processes. However, the brain-mental system has its essence in its ability to generate enough uncertainty for the environment to mean information and its executive adaptation response.

This results in a state of the matter than can be observed in two ways: 1) the statement about the null or few contributions of structural brain connectivity for the understanding of cognitive processes, calling it beautiful figures that do not deliver knowledge [26] ("just pretty pictures"); 2) the traditional structure that uses post-hoc interpretations over a factory of correlations. The tasks suitable to correlate with a DTI model will be relevant for cognitive-affective processes when variety of conditions, allow set parameter variations in the form of structured behavior samples (SBS). An acquisition and analysis that shows null physical knowledge of MR diminishes the credibility of physicists who developed the technique [25,41-44].

The lists of WMTs, next to the lists of variables, with a page of significant and non-significant correlations, cannot be structured as knowledge, but if the technological equipment is available, they are works that are published relatively easily, because they have the appearance of high complexity, and they have no difficulty, because even routine MR-DD have been published while a scale is applied when the participant, and even the patient, will enter the MR-device, also when the study has finished, which lasts between 5-8 minutes. The calculation of FA with evidence of ignorance of what it means, the signaling of WMTs that cannot be captured with the acquisition design applied, the signaling of the "robust significance" of a poor correlation that is taken from a misinterpreted conceptual framework, generates that lists of dissected WMTs without prior hypotheses: Scroll until a significant correlation is found between more than 300 variables. The big problem is that this does not generate confidence, because they are not robust results, the conditional measures associated with structural connectivity need to guarantee stability, and for that, SBSs with variations are applied until the adequate parameter is found for the individual.

JACtree and the orthotropic-radial approach will be perfected, passed, but goes to the core of "just pretty pictures for cognitive-affective knowledge". JACtree calls for the cognitivization of the WMTs. The brain-mental system does not admit the dualism that underlies both the practices of "fishing significant Pearson's" as the use of phantoms or behavioral tasks not suitable for structural connectivity. The inductive hunt implied on abuse of repeated cognitive tests as well as the use of tasks outside current cognitive models come from the same root: the sociology of science [45].

The fact that non-cooperating uniaxial motus does not obtain significant correlations while the orthotropic-radial approach obtains them with precision and theoretical advances is obvious: If a

late latin EMOTION: prefix <i>e-</i> external, <i>motus</i> , to move, an external object moving an internal one	late latin ATTENTION: <i>a</i> prefix to maintain, <i>root: tendere</i> , tension, to direct the <i>tense</i> (variable force exerted to obtain a rigid state)- <i>ion</i> , suffix of activity. The activity to direct and maintain a state, regularly rigid or centrated
classic latin AFFECT: prefix <i>ad</i> -to approach <i>afficere</i> -a fact, affectivity, the quality of a fact, in order to approach or not	classic latin EXPECTANCY: <i>ex</i> outer, came from the external ; <i>spectarum</i> - observation, to see an organized spectrum. Suffix <i>io, ia</i> passive-active (the passivity of wait for a spectrum of facts to occur due to external factors)

STOP: new discipline is required

Microstructure of Cognition



A cognitive-ontology for XXI century

Figure 25. Conceptual scheme signifying the necessity for a new discipline: the microstructure of cognition, and its corresponding cognitive-ontology

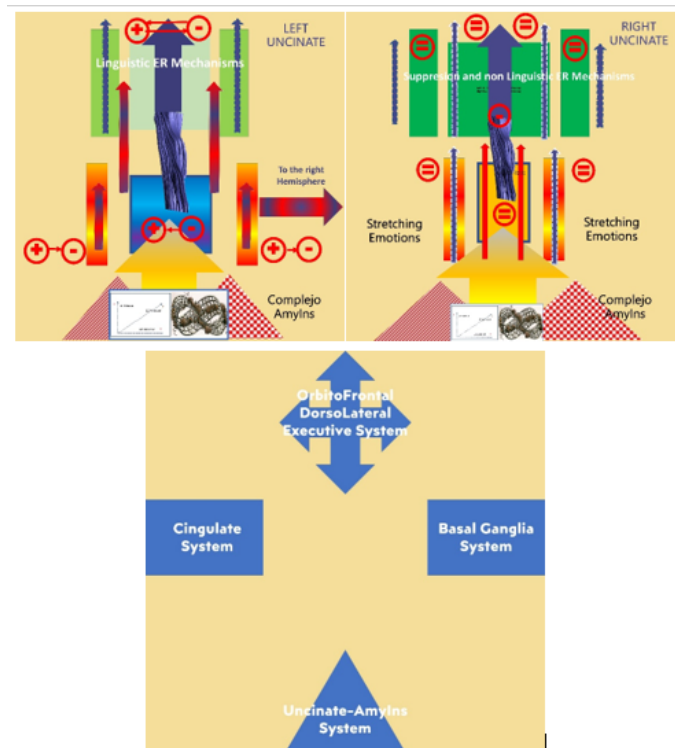


Figure 26. Integration model for the uncinate fasciculus, cingulate system and basal ganglia

heterogeneous material, which includes structural variations, is treated as a uniform bar, its signal detection is mathematically null, and statistically it will be less, anyway. This is because the radial structure of the WMTs is not a multiplication of possibilities, like over-used typical cognitive tests. The point is that WMTs effectively conduct and generate

algorithms in a complex but detectable way. Trevisiol found that at different radii of a tract ATP growth covaried detectably by Fourier transformations.

Cognitive tractography requires physicists who know how cognitive-affective processes currently follow Lisa Feldman-Barrett's "cooking recipe ingredients" models [46], the applications of Bayesian techniques by Poldrack [47], the variations of parameters that make up the Rasch with the cognitive tractography [48]. Cognitive ontologies and Diffusion Data area headache in words of their supporters (see Figure 25).

In this study, it was shown that the rigorous study of a single WMT, the UF, with the appropriate background review, with teams and people trained in both cognition-affectivity and MR physics alike, generate a model that integrates the uncinate system with the basal ganglia, the dorsal and ventral prefrontal part related to the warm-cold executive functioning and the vital "chi-square" that represents the anterior cingulate. The concept of momentum is key to understanding the uncinate system and the collected data. Momentum comes from the constructivist concept-social interaction in the production of emotions. Then a test model is generated that puts the expectation system at the center, the modulation of the value of the consequences in the face of operant behaviors, their impact on the state of mind, and the circuits of emotion production are understood both by passivity faced with a changing environment such as the conscious-unconscious, executive-by-default activity of people who have language, control proportions of events, and decrease the value of what happens or increase it depending on aspects that demand among other disciplines, to cognitive tractography. Continuing to hunt for correlations has no future, except aesthetically (Figure 26).

References

1. Catani M, Thiebaut de Schotten M (2008) A diffusion tensor imaging tractography atlas for virtual in vivo dissections. *Cortex* 44:1105–1132. [\[Crossref\]](#)
2. Mori S, Oishi K, Faria AV (2009) White matter atlases based on diffusion tensor imaging. *Curr Opin Neurol* 22: 362. [\[Crossref\]](#)
3. Catani M, Dell'Acqua F, Vergani F, Malik F, Hodge H, et al. (2012) Short frontal lobe connections of the human brain. *Cortex* 48: 273–291. [\[Crossref\]](#)
4. Catani M, Robertsson N, Beyh A, Huynh V, de Santiago Requejo F, et al. (2017) Short parietal lobe connections of the human and monkey brain. *Cortex* 97: 339–357. [\[Crossref\]](#)
5. Tax CMW, Haije T, Dela, Fuster A, Westin CF, Viergever MA, et al. (2016) Sheet Probability Index (SPI): Characterizing the geometrical organization of the white matter with diffusion MRI. *NeuroImage* 142: 260–279. [\[Crossref\]](#)
6. Kelly S, Jahanshad N, Zalesky A, Kochunov P, Agartz I, et al. (2018) Widespread white matter microstructural differences in schizophrenia across 4322 individuals: Results from the ENIGMA Schizophrenia DTI Working Group. *Mol Psychiatry* 23: 1261–1269. [\[Crossref\]](#)
7. Thiebaut de Schotten M, Dell'Acqua F, Valabregue R, Catani M (2012) Monkey to human comparative anatomy of the frontal lobe association tracts. *Cortex* 48: 82–96. [\[Crossref\]](#)
8. Mori S, Oishi K, Jiang H, Jiang L, Li X, et al. (2008) Stereotaxic white matter atlas based on diffusion tensor imaging in an ICBM template. *NeuroImage* 40: 570–582. [\[Crossref\]](#)
9. Arias JC, Marino Dávalos J, Leemans A, Caballero Bello A, Björnholm L (2019) Do neurocognitive inferences based on diffusion MRI depend on magnetic field strength and artifact correction? 5th Biological Psychiatry Symposium.
10. Marino Dávalos J, Arias JC, Jefferies E (2020) Linking individual differences in semantic cognition to white matter microstructure. *Neuropsychologia* 141: 107438.
11. Thieba C, Long X, Dewey D, Lebel C (2019) Young children in different linguistic environments: A multimodal neuroimaging study of the inferior frontal gyrus. *Brain Cognition* 134: 71–79.
12. Reynolds JE, Long X, Grohs MN, Dewey D, Lebel C (2019) Structural and functional asymmetry of the language network emerge in early childhood. *Dev Cogn Neurosci* 39: 100682. [\[Crossref\]](#)
13. Reynolds JE, Long X, Paniukov D, Bagshawe M, Lebel C (2020) Calgary Preschool magnetic resonance imaging (MRI) dataset. *Data Brief* 29: 105224. [\[Crossref\]](#)
14. Chen F, Liu T, Li J, Xing Z, Huang S, et al. (2015) Eccentric development of Balo's concentric sclerosis: detected by magnetic resonance diffusion-weighted imaging and magnetic resonance spectroscopy. *Int J Neurosci* 125: 433–440. [\[Crossref\]](#)
15. Wang C, Zhang KN, Wu XM, Huang G, Xie XF, et al. (2008) Balo's disease showing benign clinical course and co-existence with multiple sclerosis-like lesions in Chinese. *Mult Scler* 14: 418–424. [\[Crossref\]](#)
16. Trevisiol A, Saab AS, Winkler U, Marx G, Imamura H, et al. (2017) Monitoring ATP dynamics in electrically active white matter tracts. *ELife* 6: e24241. [\[Crossref\]](#)
17. Romano A, Scheel M, Hirsch S, Braun J, Sack I (2012) In vivo waveguide elastography of white matter tracts in the human brain. *Magn Reson Med* 68: 1410–1422. [\[Crossref\]](#)
18. Bach M, Laun FB, Leemans A, Tax CMW, Biessels GJ, et al. (2014) Methodological considerations on tract-based spatial statistics (TBSS). *NeuroImage* 100: 358–369. [\[Crossref\]](#)
19. Colby JB, Soderberg L, Lebel C, Dinov ID, Thompson PM, et al. (2012) Along-tract statistics allow for enhanced tractography analysis. *NeuroImage* 59: 3227–3242. [\[Crossref\]](#)
20. Lebel C, Gee M, Camicioli R, Wieler M, Martin W, et al. (2012) Diffusion tensor imaging of white matter tract evolution over the lifespan. *NeuroImage* 60: 340–352. [\[Crossref\]](#)
21. Vos SB, Jones DK, Viergever MA, Leemans A (2011) Partial volume effect as a hidden covariate in DTI analyses. *NeuroImage* 55: 1566–1576. [\[Crossref\]](#)
22. Jeurissen B, Leemans A, Sijbers J (2014) Automated correction of improperly rotated diffusion gradient orientations in diffusion weighted MRI. *Med Image Anal* 18: 953–962. [\[Crossref\]](#)
23. Leemans A, Jones DK (2009) The B-matrix must be rotated when correcting for subject motion in DTI data. *Magn Reson Med* 61: 1336–1349. [\[Crossref\]](#)
24. Van Hecke W, Leemans A, Sage Ca, Emsell L, Veraart J, et al. (2011) The effect of template selection on diffusion tensor voxel-based analysis results. *NeuroImage* 55: 566–573. [\[Crossref\]](#)
25. Leemans A, Jeurissen B, Sijbers J, Jones DK (2009) ExploreDTI: A Graphical Toolbox for Processing, Analyzing, and Visualizing Diffusion MR Data. 17th Annual Meeting of Intl Soc Mag Reson Med p: 3537.
26. Johansen-Berg H, Behrens TEJ (2006) Just pretty pictures? What diffusion tractography can add in clinical neuroscience. *Curr Opin Neurol* 19: 379–385. [\[Crossref\]](#)
27. Lebel C, Walker L, Leemans A, Phillips L, Beaulieu C (2008) Microstructural maturation of the human brain from childhood to adulthood. *NeuroImage* 40: 1044–1055.
28. Lebel C, Beaulieu C (2009) Lateralization of the arcuate fasciculus from childhood to adulthood and its relation to cognitive abilities in children. *Hum Brain Mapp* 30: 3563–3573. [\[Crossref\]](#)
29. Bassar PJ, Mattiello J, LeBihan D (1994) MR diffusion tensor spectroscopy and imaging. *Biophys J* 66: 259–267. [\[Crossref\]](#)
30. Daboul A, Ivanovska T, Bülow R, Biffar R, Cardini A (2018) Procrustes-based geometric morphometrics on MRI images: An example of inter-operator bias in 3D landmarks and its impact on big datasets. *PLoS One* 13: e0197675. [\[Crossref\]](#)
31. Nomi JS, Marshall E, Zaidel E, Biswal B, Castellanos FX, et al. (2019) Diffusion weighted imaging evidence of extra-callosal pathways for interhemispheric communication after complete commissurotomy. *Brain Struct Funct* 224: 1897–1909. [\[Crossref\]](#)
32. Carballido A, Amico F, Ugwu I, Fagan AJ, Fahey C, et al. (2012) Reduced fractional anisotropy in the uncinate fasciculus in patients with major depression carrying the met-allele of the Val66Met brain-derived neurotrophic factor genotype. *Am J Med Genet B Neuropsychiatr Genet* 159 B: 537–548. [\[Crossref\]](#)
33. Eluvathingal TJ (2006) Abnormal Brain Connectivity in Children After Early Severe Socioemotional Deprivation: A Diffusion Tensor Imaging Study. *Pediatrics* 117: 2093–2100. [\[Crossref\]](#)
34. Granger SJ, Leal SL, Larson MS, Janecek JT, McMillan L, et al. (2020) Integrity of the uncinate fasciculus is associated with emotional pattern separation-related fMRI signals in the hippocampal dentate and CA3. *Neurobiol Learn Mem* 177: 107359. [\[Crossref\]](#)

35. Sa de Almeida J, Lordier L, Zollinger B, Kunz N, Bastiani M, et al. (2020) Music enhances structural maturation of emotional processing neural pathways in very preterm infants. *NeuroImage* 207: 116391.

36. Von Der Heide RJ, Skipper LM, Klobusicky E, Olson IR (2013) Dissecting the uncinate fasciculus: Disorders, controversies and a hypothesis. *Brain* 136: 1692–1707. [\[Crossref\]](#)

37. Aldao A, Nolen-Hoeksema S, Schweizer S (2010) Emotion-regulation strategies across psychopathology: A meta-analytic review. *Clin Psychol Rev* 30: 217–237. [\[Crossref\]](#)

38. Giuliani NR, Drabant EM, Gross JJ (2011) Anterior cingulate cortex and emotion regulation: is bigger better? *Biol Psychol* 86: 379–382. [\[Crossref\]](#)

39. Gross JJ, John OP (2003) Individual differences in two emotion regulation processes: implications for affect, relationships, and well-being. *J Pers Soc Psychol* 85: 348–362. [\[Crossref\]](#)

40. Kalisch R, Buhle JT, Silvers JA, Wager TD, Lopez R, et al. (2014) Cognitive reappraisal of emotion: a meta-analysis of human neuroimaging studies. *Cereb Cortex* 24: 2981–2990. [\[Crossref\]](#)

41. Basser PJ, Pajevic S, Pierpaoli C, Duda J, Aldroubi A (2000) In Vivo Fiber Tractography. *Magn Reson Med* 44: 625–632. [\[Crossref\]](#)

42. Basser PJ, Jones DK (2002) Diffusion-tensor MRI: Theory, experimental design and data analysis - A technical review. *NMR Biomed* 15: 456–467. [\[Crossref\]](#)

43. Beaulieu C (2002) The basis of anisotropic water diffusion in the nervous system—a technical review. *NMR Biomed* 15: 435–455. [\[Crossref\]](#)

44. Mattiello J, Basser PJ, Le Bihan D (1997) The b matrix in diffusion tensor echo-planar imaging. *Magn Reson Med* 37: 292–300. [\[Crossref\]](#)

45. Bourdieu P, Passeron JC (1990) Reproduction in education, society and culture.

46. Barrett LF (2009) The future of psychology: Connecting mind to brain. *Perspect Psychol Sci* 4: 326–339. [\[Crossref\]](#)

47. Poldrack RA, Yarkoni T (2016) From brain maps to cognitive ontologies: informatics and the search for mental structure. *Annu Rev Psychol* 67: 587–612. [\[Crossref\]](#)

48. Palumbo R, Di Domenico A, Piras F, Bazzano S, Zerilli M, et al. (2020) Measuring global functioning in older adults with cognitive impairments using the Rasch model. *BMC Geriatrics* 20: 1–14.